# Influence of Time-Varying External Magnetic Fields on Trapped Fields in Bulk Superconductors

Jin Zou, *Student Member, IEEE,* Mark D. Ainslie, *Member, IEEE,* Di Hu, *Student Member, IEEE,* and David A. Cardwell

***Abstract*— Large, single-grain bulk high-temperature superconductors (HTS) can trap magnetic fields over 17 T below 30 K and up to 3 T at 77 K, and have significant potential to replace permanent magnets, the fields from which are limited to significantly less than 2 T. Therefore, bulk HTS samples are ideal candidates to develop more compact and efficient devices, such as actuators, magnetic levitation systems, flywheel energy storage systems and electric machines. In electric machines, in particular, the higher flux density improves the power density of the machine, resulting in smaller, lighter devices. However, in a real electric machine environment, bulk HTS samples can be exposed to AC magnetic field fluctuations that can affect the distribution of the supercurrent in the material and attenuate the trapped field, leading to a reduction in the magnetic loading of the machine, and in some cases, full demagnetisation. In this paper, the variation of trapped field with the frequency and magnitude of an external time-varying magnetic field is analysed numerically, and the mechanisms of the attenuation of the trapped field in HTS bulks are investigated using a two-dimensional (2D) axisymmetric finite-element model based on the *H*-formulation, considering both the electromagnetic and thermal behaviour of the bulk sample.**

***Index Terms*—High-temperature superconductors, numerical simulation, trapped field magnets, trapped field attenuation, finite element method.**

## I. Introduction

Large single-grain (RE)BCO high-temperature superconducting (HTS) bulk materials have great potential to trap high magnetic fields of over 17 T below 30 K [1], [2] and up to 3 T at 77 K [3]. Bulk HTS materials can act as permanent magnet equivalents in a number of applications, including rotating machines [4]-[7] and magnetic bearings [8]-[11]. In a trapped flux-type superconducting synchronous machine [12], where the HTS bulks act as trapped field magnets (TFMs), (RE)BCO samples can be employed in the rotor and magnetized parallel to the c-axis before the machine rotates. In these rotating machines, the position of bulk sample is expected to follow continuously the rotating field generated by the stator/armature winding. In practice, however, any ripples in the applied torque on the shaft may cause the trapped field to become misaligned with the direction of stator over a short time period [13]. Due to lateral movement or an inhomogeneous stator field, the HTS bulks may experience periodic variation of the external applied field [14], [15]. Although the most severe influence of external AC field arises when the field direction is perpendicular to the initial trapped field of HTS bulk [16], [17], the trapped field can decay or even be erased by the influence of an external time-varying field parallel to the direction of trapped field even when the amplitude is much smaller than the trapped magnetic field [16], [18].

Therefore, in this paper, the influence of external time-varying fields on trapped field attenuation is investigated to describe the magnetic behaviour of type-II superconductors subjected to AC magnetic fields whose direction is parallel to their initial magnetization [19]-[21]. In such studies performed to address the cause in the decay of trapped field, the attenuation of trapped field in HTS bulks subjected to external AC fields is attributed to the flux creep (even without an external field), shielding current redistribution within the HTS bulks [22], and AC losses generated by the penetration of the external AC field into the bulk [23]. In order to further investigate influence of each factor on HTS bulks, numerical simulations are carried out using an electromagnetic model with and without a thermal model. The modelling frameworks for electromagnetic and thermal simulations are described in Section II. The simulation results, including the influence of the frequency and magnitude of the external AC field, are presented in Section III. In addition, the thermal profile of the bulk sample is also provided to facilitate further understanding of the results from the electromagnetic-thermal model.

## II. Numerical Simulation

### A. Electromagnetic Model

The electromagnetic properties are simulated using a two-dimensional (2D) axisymmetric model based on the ***H***-formulation [24]-[31] and is solved using the Finite Element Method (FEM) implemented using COMSOL Multiphysics 4.3a. The model uses the COMSOL partial differential equation (PDE) module, and more details on the implementation can be found in [32], [33]. The E-J power law ($E \alpha J^n$) is used to simulate the non-linear electrical properties of the superconductors, where n = 21 and $E_0 = 1 \times 10^{-4}$ V/m. $J_{c0}$ is assumed to be $2 \times 10^8$ A/m$^2$, which is consistent with the

Manuscript received Aug 2, 2014. This work was supported in part by a Henan International Cooperation Grant, China: 144300510014. . M. D. Ainslie would like to acknowledge financial support from a Royal Academy of Engineering Research Fellowship. D. Hu and J. Zou would like to acknowledge financial support from Churchill College, the China Scholarship Council and the Cambridge Commonwealth, European and International Trust.

J. Zou, M. D. Ainslie, D. Hu and D. A. Cardwell are with the Bulk Superconductivity Group, Department of Engineering, University of Cambridge, Cambridge CB2 1PZ, UK (e-mail: jz351@cam.ac.uk, mark.ainslie@eng.cam.ac.uk, dh455@cam.ac.uk, dc135@cam.ac.uk)

measured material properties of the (RE)BCO bulk superconductors fabricated by the Cambridge Bulk Superconductivity Group [34].

The HTS bulk samples used in all models have a radius of 10 mm and thickness of 10 mm. The simulation is split into three time domains:

(a) $0 < t < 1$ s, pulsed field magnetisation (PFM) with an approximate 10 ms rise time and 90 ms relaxation time;
(b) $1 \leq t < x$ s, sinusoidal external magnetic field of magnitude $B_{ext}$ and frequency f is applied;
(c) $x \leq t < x + 4$ s, relaxation time of 4 s.

The HTS bulk sample is magnetised by pulsed field magnetisation (PFM) with a pulse of rise time $\tau = 0.01$ s, and a peak amplitude (annotated as $B_{pulse}$) of 1.5 T to ensure full penetration. The pulse is described by Equation (1) [35].

$$B_{pulse}(t) = \left|B_{pulse}\right| \frac{t}{\tau} \exp\ (1-\frac{t}{\tau}) \qquad (1)$$

In this ideal electromagnetic model, any increase in temperature due to the movement of flux lines [35], which is essentially a form of AC loss, is ignored.

The reduction of trapped field due to flux creep and shielding current redistribution is analysed easily in this electromagnetic model without consideration of temperature rise during the process.

### B. Thermal Model

In order to simulate the thermal effect of an external field on trapped field, a thermally-isolated bulk model is used to simulate the thermal properties. The bulk sample is assumed to be surrounded by liquid nitrogen to provide a uniform, ambient temperature of 77 K. The simulation is carried out using the COMSOL Heat Transfer module, coupled with the ***H***-formulation. More details of model coupling can be found in [35]. The bulk sample is first magnetised, then exposed to the same external field as described in the previous section.

Trapped field decay resulting from temperature rise, which is generated by the AC losses, is indicated by the difference between the electromagnetic and combined electromagnetic-thermal models.

## III. Modelling Results

### A. Frequency influence on trapped field

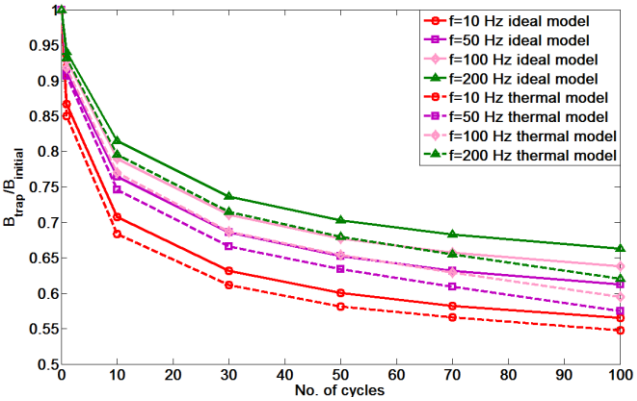


Fig. 1. Influence of frequency on attenuation of trapped field varying with cycles for $B_{ext} = 0.2$ T.

In Fig 1, $x$ in the model equals to the time required for particular number of cycles of external AC field applied to the sample.

$$x = nT \qquad (2)$$

where $n$ is the number of cycles of applied field and $T$ is the period of the field. The other time domains are the same as described in Section II.A, including 1 s initially for PFM, then 4 s of relaxation time after the required number of cycles of external AC field is applied, as shown in Fig. 1.

Fig. 1 shows the ratio of trapped field, $B_{trap}$, with number of cycles of applied external AC field, to the initial trapped field, $B_{initial}$. This is calculated 0.5 mm above the centre of the top surface of the bulk, using the models described in Sections II.A and B with $B_{ext} = 0.2$ T. For the electromagnetic model only, the initial trapped field after PFM is $B_{initial} = 0.47$ T. However, for the thermal model, $B_{initial}$ decreases to 0.42 T due to the temperature rise during the PFM process.

These trends are also observed in experiments [36], [37]. The attenuation of trapped magnetic field over a short time (based on number of cycles) decreases with increasing frequency of external field in both models. Considering only the ideal electromagnetic model, this decay of trapped field is attributed to flux creep and the redistribution of the shielding current in the bulk due to penetration of the external magnetic field [37]. In the area penetrated by the external field, the screening current cannot effectively contribute to the trapped field and reduces the overall trapped field [21], [38].

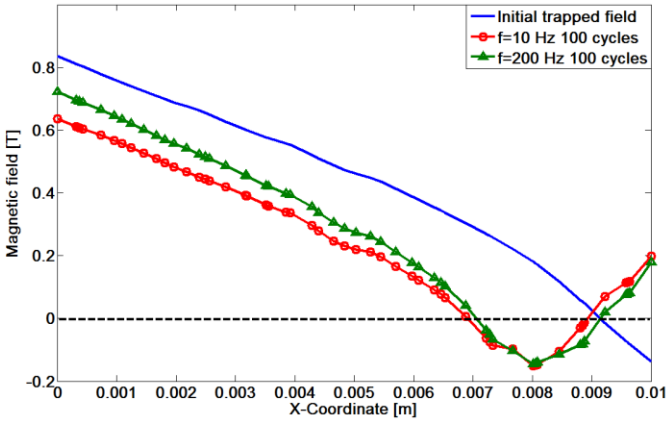


Fig. 2. Comparison of trapped field in the bulk superconductor across the centre (z = 0 m) for f = 10 Hz and f = 200 Hz for $B_{ext} = 0.2$ T.

The higher the frequency of the applied AC field, the lower attenuation in the trapped field per cycle due to the lower penetration depth. Fig. 2 shows the penetration depth for f = 10 Hz and f = 200 Hz, where the trapped field is recorded along the middle plane of the sample (z = 0 m). The penetration depth decreases with increasing frequency of external field. The difference in penetration depth becomes more obvious with an increasing number of cycles. Thus, it can be considered that for higher frequency of AC external field, the penetration depth into the bulk sample is lower and a larger proportion of undisturbed supercurrent contributes to trapped field.

Comparing the models in Fig. 1, in the case of f = 200 Hz, the difference in the ideal and thermal models is more obvious than for f = 10 Hz. This difference represents the thermal effect on the bulk sample. The thermal effect is more pronounced for higher frequencies and the trapped field can decreases severely (e.g., f = 200 Hz). However, the remanent trapped field in the thermal model, even for the high frequency case (say 200 Hz), is still relatively high compared to the low frequency case (10 Hz) over 100 cycles. Therefore, the influence per cycle is dominated more by the penetration depth of the external field in this case.

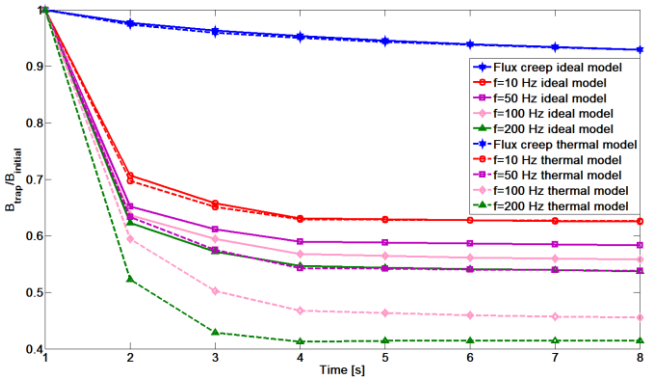


Fig. 3. Influence of frequency on attenuation of trapped field varying with time for $B_{ext}$ = 0.2 T.

The results for the decay of trapped field per cycle are limited, and observing the decay using a time scale, rather than cycles, gives another viewpoint. In order to compare the result using a time scale, we set x = 4 s for the following analyses. The other settings are the same as Section II.A and Fig. 3 shows the trapped fields calculated every second by this same method.

The attenuation caused by flux creep, which depends largely on the n value of the bulk sample, is quite different from that caused by an external AC field. Although decay of trapped field per cycle is low for high frequency scenario (Fig. 1), the total attenuation over time increases with frequency due to an increased number of cycles per second (Fig. 3) in models both electromagnetic and thermal models.

Compared with the results shown in Fig. 1, the difference between the ideal and thermal models is enlarged using a time-based scale (see Fig. 2), and the thermal effect is more prominent in this case. In addition to the supercurrent redistribution and flux creep, there is also a contribution to the decay of trapped field from the AC loss, which reduces the critical current density by increasing the local temperature. Therefore, the attenuation of trapped field for higher frequency is larger, because flux movement of high frequency generates a more substantial AC loss over a small area, within which the temperature will increase considerably and rapidly, which is analysed in more detail in Section III B. The temperature rise decreases the critical current density in the bulk sample, further accelerating the reduction in the trapped field. Therefore, thermal effects are significant when considering longer time periods.

Without thermal effects, the difference in the penetration depth makes attenuation of the trapped field more severe for low frequencies. Including the thermal effect, the temperature rise decreases the trapped field significantly in the high frequency case.

### *B. Thermal profile influence*

In order to investigate the temperature rise due to the heat generated during the simulation, thermal profiles of two points (the centre and edge points) of the HTS bulk sample are investigated, as shown in Fig. 4.

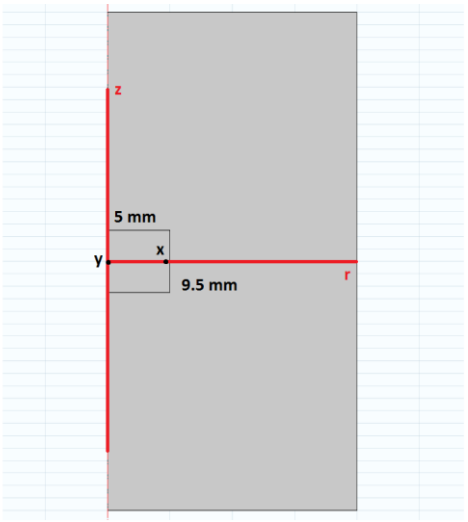


Fig. 4. Axisymmetric geometry of the HTS bulk, including points x and y for thermal analysis.

The point x is 0.5 mm inside of the bulk sample from the edge (r = 9.5 mm, z = 0 mm), and the centre point is y (r = 0 mm, z = 0 mm), and the observed temperature changes for these points are shown in Figs. 5 and 6.

The temperature profiles of points x and y during the application of the external AC field (f = 50 Hz, $B_{ext}$ = 0.2 T, from 1 s to 8 s) are shown in Figs. 5 and 6. The temperature rise is larger for higher frequencies for both points. As discussed in Section III A, the trapped field decays significantly in the case of f = 200 Hz, which also has a higher temperature rise (see Figs. 5 and 6).

In Fig. 6, at point x, the temperature immediately increases when the AC field is applied. However, the temperature of point y starts to rise around t = 1.5 s due to heat diffusion from the outer to inner area of the sample. For the point at the edge x, the temperature has a peak at t = 4s and after 4 s the temperature drops slightly. However, for point y the peak temperature value occurs at t = 5 s, which could be due to the heat diffusion also. The exact mechanisms of this temperature behaviour at points x and y should be investigated in detail in future work.

Fig. 7 shows the temperature distribution from the end of first cycle to the end of applied AC field (t = 4 s) with varying frequency (f = 10 Hz to f = 200 Hz). At the end of the first cycle, the temperature change is almost the same for all frequencies. For f = 10 Hz, the temperature approximately remains constant with external AC field. However, at t = 4 s, with increasing frequency, the temperature rise increases. In addition, heat is generated from the edge and transfers laterally to the centre of the bulk as shown. The results shown in Fig. 7 agree well with those of Figs. 5 and 6.

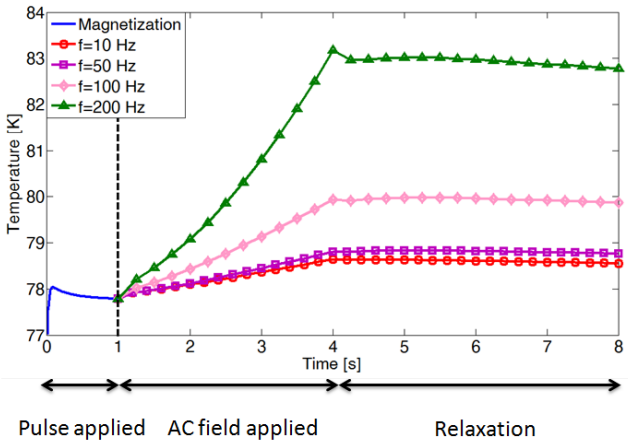


Fig. 5. Temperature profile for point x with varying frequency.

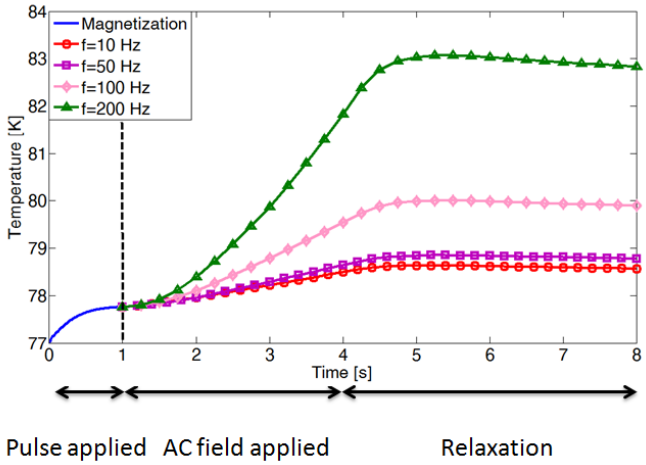


Fig. 6. Temperature profile for point y with varying frequency.

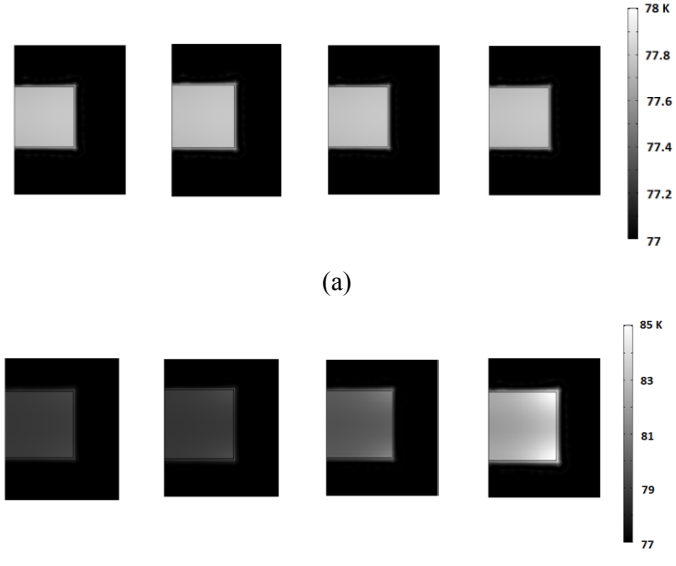


Fig. 7. (a) Temperature profiles from the end of the first cycle for increasing frequency (10, 50, 100 and 200 Hz, from left to right, respectively), (b) Temperature profile at the end of applied AC field (t = 4 s).

### C. *Influence of external applied field amplitude*

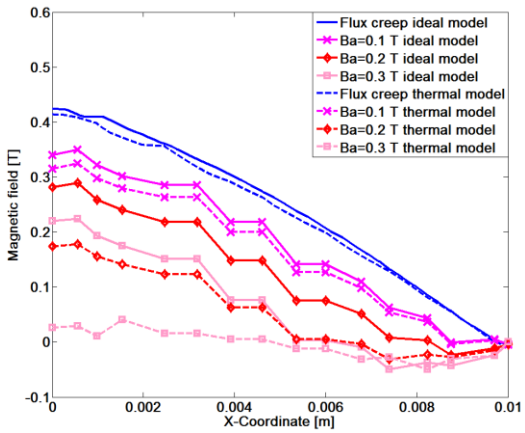


Fig. 8 Influence of external applied field amplitude on attenuation of trapped field at t = 8 s.

The influence of the external applied field amplitude $B_{ext}$ for f = 50 Hz is shown in Fig. 8. Although the decay of trapped field due to increased temperature is not obvious for $B_{ext}$ = 0.1 T, the trapped field is almost erased, when it exposes to 0.3 T AC field with thermal model. The results agree well with the experimental results presented in [16], [18].

## IV. Conclusion

HTS bulk superconductors are ideal candidates to develop more compact and efficient devices, such as actuators, magnetic levitation systems, flywheel energy storage systems and electric machines, due to their ability to trap large magnetic fields. In this paper, the effect of AC magnetic field fluctuations on the attenuation of the trapped field in HTS bulks was investigated numerically.

Electromagnetic and combined electromagnetic-thermal 2D axisymmetric bulk models were used to investigate the influence of the frequency and magnitude of an external AC field on the trapped field profile. Without the inclusion of thermal effects, it was found that the larger penetration depth for lower frequencies causes greater attenuation of the trapped field. However, when including the thermal model, the higher temperature rise for higher frequencies decreases the trapped field significantly. Finally, larger magnitudes of external field can attenuate the trapped field severely, including cases where the trapped field in the bulk material is almost erased by relatively higher magnitudes of AC field, for the cases studied.

These results help better explain the main effects – with regard to penetration depth, redistribution of supercurrent and AC losses – of time-varying external fields on the trapped fields of HTS bulk samples.

## Acknowledgment

Di Hu and Jin Zou would like to acknowledge the support of Churchill College, Cambridge, the China Scholarship Council and the Cambridge Commonwealth, European and International Trust. Dr Mark Ainslie would like to acknowledge the support of a Royal Academy of Engineering Research Fellowship. This work was supported in part by a Henan International Cooperation Grant, China: 144300510014.

## REFERENCES


[1] M. Tomita, and M. Murakami, "High-temperature superconductor bulk magnets that can trap magnetic fields of over 17 tesla at 29 K," *Nature*, vol. 421, pp. 517–520, Jan. 2003.

[2] J. H. Durrell *et al.*, "A trapped field of 17.6 T in melt-processed, bulk Gd-Ba-Cu-O reinforced with shrink-fit steel," *Supercond. Sci. Technol.*, vol. 27, pp. 082001, Aug. 2014.

[3] S. Nariki, N. Sakai, and M. Murakami, "Melt-processed Gd-Ba-Cu-O superconductor with trapped field of 3 T at 77 K," *Supercond. Sci. Technol.*, vol. 18, pp. S126–S130, Feb. 2005.

[4] B. Oswald *et al.*, "Reluctance motors with bulk HTS material," *Supercond. Sci. Technol*, vol. 18, pp. S24–S29, Feb. 2005.

[5] X. Granados, *et al*., "Low-power superconducting motors," *Supercond. Sci. Technol.* vol. 21, pp. 034010, Mar. 2008.

[6] Y. Jiang *et al.*, "The design, magnetization and control of a superconducting permanent magnet synchronous motor," *Supercond. Sci. Technol.* vol. 21, pp. 065011, Jun. 2008.

[7] P. J. Masson, *et al.*, "Design of HTS axial flux motor for aircraft propulsion," *IEEE Trans. Appl. Supercond.* vol.17, pp. 1533-1536, Jun. 2007.

[8] J. R. Hull, "Superconducting bearings," *Supercond. Sci. Technol.* vol. 13, no. 2, Feb. 2000

[9] H. Sino, K. Nagashima, and Y. Arai, "Development of superconducting magnetic bearing using superconducting coil and bulk superconductor," *J. Phys.: Conf. Ser.*, vol. 97, pp. 012101, 2008.

[10] N. Koshizuka, "R&D of superconducting bearing technologies for flywheel energy storage systems," *Physica C*, vol. 445–448, pp. 1103, Oct. 2006.

[11] F. N. Werfel, "HTS magnetic bearings," *Physica C*, vol. 372–376, pp. 1482, Aug. 2002.

[12] H. Matsuzaki *et al*., "An axial gap-type HTS bulk synchronous motor excited by pulsed-field magnetization with vortex-type armature copper windings," *IEEE Trans. Appl. Supercond.* vol. 15, pp. 2222–2225, Jun. 2005.

[13] M. Qiu *et al*., "Technical analysis on the application of HTS bulk in "permanent magnet" motor," *IEEE Trans. Appl. Supercond*., vol. 15, pp. 3172–3175, Jun. 2005.

[14] M. Qiu *et al*., "Electromagnetic phenomena in HTS bulk subjected to a rotating field," *IEEE Trans. Appl. Supercond.* vol. 14, pp. 1989–1991, Jun. 2004.

[15] G. T. Ma *et al*., "Method to reduce levitation force decay of the bulk HTSC above the NdFeB guideway due to lateral movement," *Supercond. Sci. Technol*., vol. 21, pp. 065020, Jun. 2008.

[16] J. Ogawa et al., "Influence of AC external magnetic field perturbation on trapped magnetic field in HTS bulk," *Physica C*, vol. 386, pp. 26–30, Apr. 2003.

[17] P. Vanderbemden *et al*., "Behavior of bulk high-temperature superconductors of finite thickness subjected to crossed magnetic fields: Experiment and model," *Phys. Rev. B*, vol. 75, pp. 174515, May 2007.

[18] K. Yamagishi, J. Ogawa, O. Tsukamoto, M. Murakami, and M. Tomita, "Decay of trapped magnetic field in HTS bulk caused by application of AC magnetic field," *Physica C*, vol. 392-396, pp.659 -663,Oct. 2003.

[19] O. Tsukamoto *et al.* "Mechanism of decay of trapped magnetic field in HTS bulk caused by application of AC magnetic field," *J. Mater. Process Tech.*, vol. 161, pp. 52–7, Apr. 2005.

[20] A. Ninomiya *et al*., "An experimental study on decay characteristics of magnetized flux in YBCO-QMG bulk material under AC magnetic field," *IEEE Trans. Appl. Supercond*., vol. 18, no.2, pp. 1362–1365, Jun. 2008.

[21] J. Ogawa *et al.*, "Influence of high frequency AC magnetic field on trapped magnetic field," *IEEE Trans. Appl. Supercond*., vol. 17, pp. 3024–3027, Jun. 2007.

[22] H. Ueda *et al*., "Trapped field characteristic of HTS bulk in AC external magnetic field," *IEEE Trans. Appl. Supercond.*, vol. 13, pp. 2283–2286, Jun. 2003.

[23] Y. Zushi *et al*., "Study on suppression of decay of trapped magnetic field in HTS bulk subject to AC magnetic field," *Physica C*, vol. 412, pp. 708–713, Oct. 2004.

[24] Comsol, Inc. http://www.comsol.com

[25] M. D. Ainslie *et al*., "Numerical analysis and finite element modelling of an HTS synchronous motor," *Physica C*, vol. 470, pp. 1752–1755, Nov. 2010.

[26] M. D. Ainslie *et al*., "Comparison of first-and second-order 2D finite element models for calculating AC loss in high temperature superconductor coated conductor," *Int. J. Comput. Math. Electr. Electron. Eng.*, vol. 30, pp. 762–774, 2011.

[27] M. D. Ainslie, T. J. Flack, and A. M. Campbell, "Calculating transport AC losses in stacks of high temperature superconductor coated conductors with magnetic substrates using FEM," *Physica C*, vol. 472, pp. 50–56, Jan. 2012.

[28] M. D. Ainslie *et al*., "An improved FEM model for computing transport AC loss in coils made of RABiTS YBCO coated conductors for electric machines", *Supercond. Sci. Technol*., vol. 24, pp. 045005, Apr. 2011.

[29] Z. Hong, A. M. Campbell, and T.A. Coombs, "Numerical solution of critical state in superconductivity by finite element software," *Supercond. Sci. Technol.*, vol. 19, pp.1246–1252, Dec. 2006.

[30] Z. Xu *et al*., "Theoretical simulation studies of pulsed field magnetisation of (RE) BCO bulk superconductors," *J. Phys.: Conf. Ser*, vol. 234, pp. 012049, 2010.

[31] Z. Hong, A.M. Campbell, and T. A. Coombs. "Computer modeling of magnetisation in high temperature bulk superconductors," *IEEE Trans. Appl. Supercond.*, vol. 17, pp. 3761–3764, Jun. 2007.

[32] M. Zhang *et al*., "Experimental and numerical study of a YBCO pancake coil with a magnetic substrate," *Supercond. Sci. Technol.*, vol. 25, pp. 125020, Dec. 2012.

[33] A. Patel, and B. A. Glowacki, "Enhanced trapped field achieved in a superconducting bulk using high thermal conductivity structures following simulated pulsed field magnetization," *Supercond. Sci. Technol.*, vol. 25, pp. 125015, Dec. 2012.

[34] Z. Xu *et al*., "Simulation studies on the magnetization of (RE)BCO bulk superconductors using various split-coil arrangements," *Supercond. Sci. Technol.*, vol. 25, pp. 025016, 2012.

[35] M. D. Ainslie *et al*., "Modelling and comparison of trapped fields in (RE)BCO bulk superconductors for activation using pulsed field magnetization," *Supercond. Sci. Technol.*, vol. 27, pp. 065008, Apr. 2014.

[36] T. Ohyama *et al.*, "Trapped field characteristics of Y-Ba-Cu-O bulk in time-varying external magnetic field," *IEEE Trans. Appl. Supercond.*, vol. 11, pp. 1988–1991, Mar. 2001.

[37] H. Ueda, M. Itoh, and A. Ishiyama, "Trapped field characteristic of HTS bulk in AC external magnetic field," *IEEE Trans. Appl. Supercond.*, vol. 13, pp. 2283–2286, Jun. 2003.

[38] O. Tsukamoto *et al.*, "Mechanism of decay of trapped magnetic field in HTS bulk caused by application of AC magnetic field," *J. Mater. Proc. Technol.*, vol. 161, pp. 52–57, Apr. 2005.